Search for the minimum thermal conductivity in mixed cryocrystals $(CH_4)_{1-\xi}Kr_\xi$

V. A. Konstantinov[1], V. G. Manzhelii[1], R. O. Pohl[2], and V. P. Revyakin[1]

[1] B. Verkin Institute for Low Temperature Physics and Engineering of the National Academy of Sciences of Ukraine
47 Lenin ave., Kharkov, 63103, Ukraine
E-mail: konstantinov@ilt.kharkov.ua

[2] Laboratory of Atomic and Solid State Physics, Cornell University, Ithaca, New York, USA

The isochoric thermal conductivity of $(CH_4)_{1-\xi}Kr_\xi$ solid solutions is studied between 40 K and ~ 150 K over the wide range of concentrations ($\xi = 0.013$, 0.032, 0.07, 0.115, 0.34, 0.71, 0.855, 0.937, and 0.97). A gradual transition from the thermal conductivity of a highly perfect crystal to the minimum thermal conductivity is observed as the crystal becomes increasingly more disordered. A qualitative description is given in the framework of Debye model of thermal conductivity, which takes into consideration the fact that phonon mean free path cannot decrease indefinitely.

Introduction

The question of what occurs when the mean free path of a phonon becomes comparable to the lattice parameter or to its own wavelength is one of the most intriguing problems in the thermal conductivity of solids [1–6]. Some progress in the description of the heat transport in strongly disordered materials has come about through the concept of the minimum thermal conductivity Λ_{min} [4–6], which is based on the picture where the lower limit of the conductivity is reached when the heat is being transported through a random walk of the thermal energy between the neighboring atoms or molecules vibrating with random phases. In this case Λ_{min} can be written as the following sum of three Debye integrals [5,6]:

$$\Lambda_{min} = \left(\frac{\pi}{6}\right)^{1/3} k_B n^{2/3} \sum_i v_i \left[\left(\frac{T}{\Theta_i}\right)^2 \int_0^{\theta_i/T} \frac{x^3 e^x}{(e^x - 1)^2}\, dx \right].$$

$$(1)$$

The summation is taken over three (two transverse and one longitudinal) sound modes with the sound speeds v_i, Θ_i is the Debye cutoff frequency for each polarization expressed in degrees Kelvin, $\Theta_i = v_i(\hbar/k_B)(6\pi^2 n)^{1/3}$, and n is the number density of atoms or molecules. Although no theoretical justification exists as yet for this picture of the heat transport, evidence for its validity has been obtained on a number of amorphous solids in which the high-temperature thermal conductivity has been found to agree with the value predicted by this model [5]. Indirect evidence has also been obtained in measurements of the thermal conductivity of highly disordered crystalline solids, in which no thermal conductivity smaller than that predicted by this model seems to have ever been observed [6]. What has been missing so far, however, has been a systematic study of the gradual transition from the thermal conductivity of a highly perfect crystal to the minimum thermal conductivity as the crystal becomes increasingly disordered. Such measurements will be presented here.

The objects of this study were $(CH_4)_{1-\xi}Kr_\xi$ solid solutions ($0 \leq \xi \leq 1$). This choice was based on the following considerations, i.e.,

i) The phase diagram of $(CH_4)_{1-\xi}Kr_\xi$ has been studied quite well. It was found that the components form a homogeneous solid solution with fcc structure above 30 K at all ξ [7].

ii) Kr and CH_4 have similar molecule/atom radii and parameters of the pair potential [8]. The

Debye temperatures Θ_D of Kr and CH_4 are 72 and 143 K, respectively [7,8]. At the same time the masses of the Kr atom and the CH_4 molecule are very different, 83.8 and 16 atomic units, respectively. The fractional mass difference $\Delta M/M$ is 0.81 for the CH_4 impurity in Kr and 4.23 for the Kr impurity in methane. One can thus expect strong impurity scattering, especially in the latter case.

iii) The peculiarities of the heat transfer in pure Kr and CH_4 have been studied in detail (Refs. 9–12 and 13–15, respectively). There have been separate studies of the low-temperature thermal conductivity at $T < 20$ K in the mixed cryocrystals, which indicate strong point-defect scattering [12,15]. The thermal conductivity Λ_{meas}^P of solid CH_4 and Kr measured at the saturated vapor pressure is shown in Fig. 1 together with Λ_{min}, calculated by Eq. (1) for equilibrium conditions. The corresponding values of the density and sound velocities at different temperatures needed for the calculation were taken from Refs. 8 and 16. As can be seen from Fig. 1 the thermal conductivity of Kr goes through a maximum at 12 K and then decreases, approaching its lower limit Λ_{min} at premelting temperatures. The thermal conductivity of CH_4 goes through a maximum at 4.5 K in the orientationally ordered α phase and decreases subsequently to the α–β transition temperature $T_{\alpha-\beta} = 20.4$ K. In the orientationally disordered (OD) β phase the thermal conductivity begins to increase again, goes through another maximum at 50 K, and then decreases as far as the melting-point temperature $T_m = 89.8$ K. The ratio $\Lambda_{meas}^P/\Lambda_{min}$ is shown in Fig. 2. It is seen that Λ_{meas}^P exceeds the lower limit Λ_{min} by a factor of two to four in the entire region of the OD phase.

For these reasons, the $(CH_4)_{1-\xi}Kr_\xi$ mixed cryocrystals enable us to study the influence of atomic-size defects upon the thermal conductivity near its

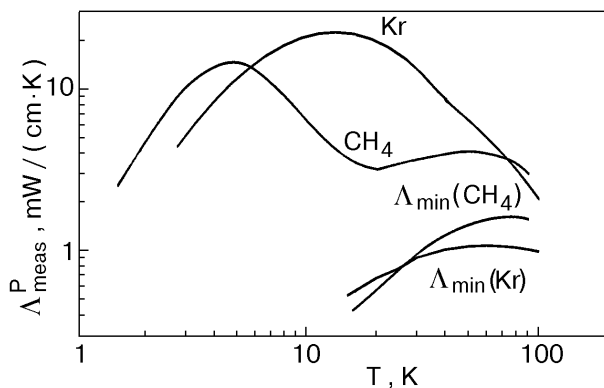*Fig. 1.* The thermal conductivities Λ_{meas}^P of solid Kr and CH_4 measured at saturated vapor pressures according to data of Refs. 9–15. Λ_{min} of solid Kr and CH_4 calculated by Eq. (1) are shown at the bottom.
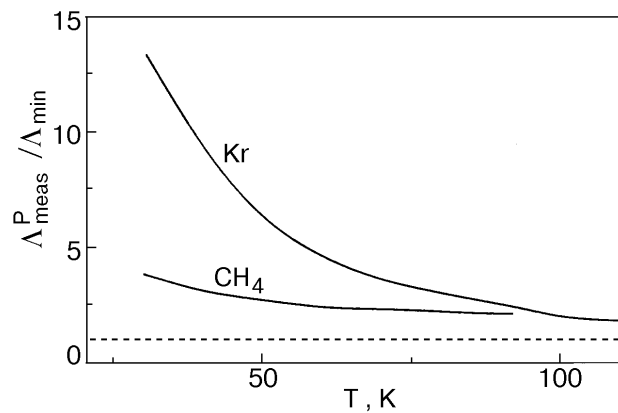

Fig. 2. The ratio $\Lambda_{meas}^P/\Lambda_{min}$ for solid Kr and CH_4. The dashed line corresponds to $\Lambda_{meas}^P/\Lambda_{min} = 1$.

lower limit and to test the validity of the concept of the minimum thermal conductivity in the form it was reported in [5,6].

Experimental technique

To compare correctly experimental results of thermal conductivity with theory at $T \geq \Theta_D$ it is necessary to perform experiments at constant density to exclude the effect of thermal expansion. The simplest molecular crystals and solidified inert gases are best suited, since their thermal expansion coefficients are much larger than those of the materials commonly used in high-pressure cells. If a high-pressure cell is filled with a solid sample of quite high density, on subsequent cooling the volume of the sample will remain practically constant while the pressure of the sample decreases. The small deviations from the constant volume caused by thermal and elastic deformation of the measuring cell can easily be taken into account.

The V–T diagram of solid Kr plotted according to data of Ref. 16 is shown in Fig. 3. As an example, two isochores are shown, which correspond to the volumes 28.5 and 29.0 $cm^3/mole$. T_0 is the temperature at which the $V = const$ condition comes into play in the experiment. Below T_0 the isochoric data convert to the data measured at saturated vapor pressure, and on further cooling the sample can pull away from the cell walls. The temperature T_m and pressure P_m correspond to the onset of sample melting. T_0 and T_m shift towards lower and higher temperature as the density of the sample increases.

The molar volume of $(CH_4)_{1-\xi}Kr_\xi$ solid solution varies appreciably (about 10% at the saturated vapor pressure) as a function of the component

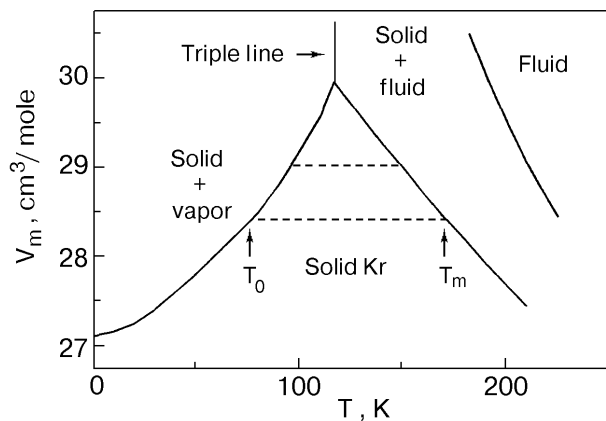*Fig. 3.* The V–T diagram for solid Kr according to Ref. 16. The two isochores are shown, which correspond to the volumes 28.5 and 29.0 cm^3/mole.

concentrations [7]. In this context it is convenient to compare the experimental results taken at different concentrations for those samples which reach the $V = \text{const}$ condition at the same temperature T_0. There are certain experimental difficulties to prepare the samples with the same temperature T_0. However, if the thermal conductivity is studied on several isochores at the same concentration of the components, it can be recalculated to any T_0, using the volume dependence of thermal conductivity in the form: $g = -(\partial \ln \Lambda / \partial \ln V)_T$, where g is the Bridgman coefficient. Since the pressure at temperature T_0 is zero, $\Lambda(T_0)$ corresponds to the isobaric thermal conductivity $\Lambda_P(P = 0)$ as well.

This study was carried out on a coaxial-geometry setup, using the steady-state method. The measuring beryllium bronze cell (160 mm long, 17.6 mm inner diameter) was engineered for a maximum pressure of 800 MPa. The inner measuring cylinder was 10.2 mm in diameter. The sample was between the outer and the inner cylinder. The temperature was measured with platinum resistance thermometers, mounted in special channels of the inner and outer cylinders and unaffected by high pressure. During the sample growth, a temperature gradient ~ 1 K/cm was maintained along the measuring cell. The pressure in the inlet capillary and the cell was produced by a special thermocompressor, and was varied from 50 to 250 MPa for obtaining samples of various densities. Under identical growing conditions (a capillary pressure ≈ 200 MPa and a temperature gradient along the cell ≈ 1 K/cm) we were able to prepare denser samples of solid solutions with CH$_4$ prevailing ($\xi < 0.3$) than with Kr prevailing. This may be due to the higher compressibility of CH$_4$ as compared to that of Kr. When the

sample growth was completed, the inlet capillary was blocked at liquid hydrogen temperature and the samples were annealed at premelting temperatures for 5–6 h to remove density gradients. After completion of the experiment the samples were evaporated into a thin-wall vessel and their masses were determined by weighing. The molar volumes of the samples were estimated from the known volume of the measuring cell and from the sample mass. The total systematic error was dominant, but did not exceed 4% for the thermal conductivity and 0.2% for molar volume. The purity of the Kr and CH$_4$ gases used was better than 99.98%. The experimental details are described more comprehensively in Ref. 17.

Results

The smoothed coefficients of isobaric Λ_P and isochoric Λ_V thermal conductivities are presented in Tables 1 and 2. The molar volumes V_m of the samples, the temperatures T_0 at which the $V = \text{const}$ condition comes into play in the experiment, and the temperatures T_m of the beginning of sample melting are given in Table 3 along with the Bridgman coefficients $g = -(\partial \ln \Lambda / \partial \ln V)_T$ calculated from the measured results. The isochoric thermal conductivity of pure Kr [11] and solid solution $(CH_4)_{1-\xi}Kr_\xi$ with Kr prevailing ($\xi > 0.7$) rescaled to $T_0 = 75$ K is shown in Fig. 4 together with low-temperature data [12]. Figure 5 shows the isochoric thermal conductivity of pure CH$_4$ [13] and of the solid solution with CH$_4$ prevailing ($\xi < 0.35$), rescaled to $T_0 = 40$ K, together with low-temperature data [15]. Although there is a temperature gap between the two sets of data, one can conclude that they agree quite well. The lower limits of the isochoric thermal conductivity Λ_{min} of pure Kr and CH$_4$ are shown in Figs. 4 and 5 as broken lines. The molar volumes and sound velocities needed for the calculation were taken to correspond to the temperature T_0 from Refs. 8, 16 and were assumed to be independent of temperature. For the crystals with Kr prevailing ($\xi \geq 0.97$), the isochoric thermal conductivity increases steeply as the temperature decreases. As ξ decreases, the thermal conductivity decreases as a whole and increases less steeply with decreasing temperature. At $0.3 \geq \xi \geq 0.7$ the thermal conductivity becomes practically temperature independent, as expected for the lower limit of the thermal conductivity Λ_{min} at $T \geq \Theta_D$. The measured data lie between the predicted Λ_{min} for pure Kr and CH$_4$, calculated according to Eq. (1). As ξ decreases further (CH$_4$-rich crystal), the thermal conductivity increases again, and it ap-

Table 1

Smoothed values of the isobaric Λ_P and isochoric Λ_V coefficients of thermal conductivity of the $(CH_4)_{1-\xi}Kr_\xi$ solid solution ($\xi > 0.7$) in mW/(cm·K). Molar volumes of the samples are given in cm^3/mole

T, K	$\xi = 0.97$				$\xi = 0.937$				$\xi = 0.855$			$\xi = 0.71$		
	Λ_P	Λ_V at V_m			Λ_P	Λ_V at V_m			Λ_P	Λ_V at V_m		Λ_P	Λ_V at V_m	
		28.5	28.9	29.5		28.82	29.31	29.72		29.25	29.85		29.75	30.30
40	3.60				2.75									
50	3.00				2.50									
60	2.93				2.30									
70	2.60				2.12									
80	2.30	2.43			1.85	1.88			1.5	1.5		1.05	1.08	
90	2.00	2.32	2.08		1.65	1.84			1.4	1.49		1.03	1.12	1.03
100	1.72	2.20	1.95	1.72	1.46	1.80	1.61		1.26	1.48	1.34	1.02	1.15	1.05
110	1.45	2.10	1.85	1.60	1.28	1.75	1.58	1.41	1.18	1.47	1.32	1.00	1.19	1.08
120		1.98	1.74	1.50		1.70	1.52	1.38		1.46	1.31		1.22	1.12
130		1.90	1.62	1.38		1.67	1.50	1.36		1.45	1.30		1.25	
140		1.82	1.52	1.25		1.65	1.48			1.45			1.28	
150		1.73	1.40			1.63	1.46							
160		1.68				1.60								

Table 2

Smoothed values of the isobaric Λ_P and isochoric Λ_V coefficients of thermal conductivity of the $(CH_4)_{1-\xi}Kr_\xi$ solid solution ($\xi < 0.4$) in mW/(cm·K). Molar volumes of the samples are given in cm^3/mole

T, K	$\xi = 0.011$				$\xi = 0.032$			$\xi = 0.07$				$\xi = 0.115$			$\xi = 0.34$	
	Λ_P	Λ_V at V_m			Λ_P	Λ_V at V_m		Λ_P	Λ_V at V_m			Λ_P	Λ_V at V_m		Λ_P	Λ_V at V_m
		31.03	31.60	32.05		31.00	31.62		30.85	31.42	31.80		30.70	31.22		30.50
40	2.20				2.05			1.83	1.85			1.30	1.32			
50	2.40	2.55			2.18	2.30		1.95	2.14			1.45	1.55		1.2	1.2
60	2.50	2.75			2.25	2.50		2.05	2.37	2.11		1.53	1.70	1.56	1.2	1.3
70	2.52	2.90	2.70		2.28	2.65	2.38	2.12	2.55	2.30		1.55	1.80	1.65	1.2	1.35
80	2.52	3.02	2.80	2.55	2.29	2.74	2.48	2.15	2.65	2.40	2.20	1.56	1.85	1.72	1.22	1.40
90	2.50	3.05	2.87	2.60	2.29	2.78	2.53	2.17	2.70	2.45	2.26	1.56	1.88	1.75	1.22	1.45
100		3.07	2.87	2.60		2.80	2.55		2.72	2.48	2.28		1.90	1.76		1.48
110		3.05	2.85			2.80	2.55		2.72	2.48			1.90	1.75		1.50
120		3.02				2.80	2.55		2.70				1.88			1.51
130									2.68				1.88			

Table 3

Molar volumes V_m of the samples, temperatures T_0, at which the experiment reaches the condition $V = const$, the temperatures T_m of the onset of sample melting, and the Bridgman coefficients $g = -(\partial \ln \Lambda / \partial \ln V)_T$

ξ	Number of the sample	V_m, cm³/mole	T_0, K	T_m, K	g
0.013	1	31.03	45	125	
	2	31.60	63	114	4.8
	3	32.05	79	103	
0.032	1	31.0	44	126	
	2	31.62	65	111	4.2
0.07	1	30.85	37	130	
	2	31.42	60	115	4.2
	3	31.80	72	108	
0.115	1	30.70	35	130	
	2	31.22	55	118	3.9
0.34	1	30.50	49	135	3.8
0.71	1	29.75	70	144	
	2	30.30	86	125	4.2
0.855	1	29.25	75	148	
	2	29.85	95	130	5.2
0.937	1	28.82	77	158	
	2	29.31	92	145	7.7
	3	29.72	102	133	
0.97	1	28.5	72	168	
	2	28.95	86	154	8.5
	3	29.5	100	140	

proaches that of pure CH_4 as the concentration of Kr decreases to zero. The concentration dependence of the thermal conductivity of the $(CH_4)_{1-\xi}Kr_\xi$ solid solution at $T = 75$ K and $P = 0$ is shown in Fig. 6. The Λ_{min} of pure Kr and CH_4 are shown as broken lines. It is seen that thermal conductivity changes rapidly at $\xi < 0.2$ and $\xi > 0.8$ and is practically concentration independent at $0.2 < \xi < 0.8$.
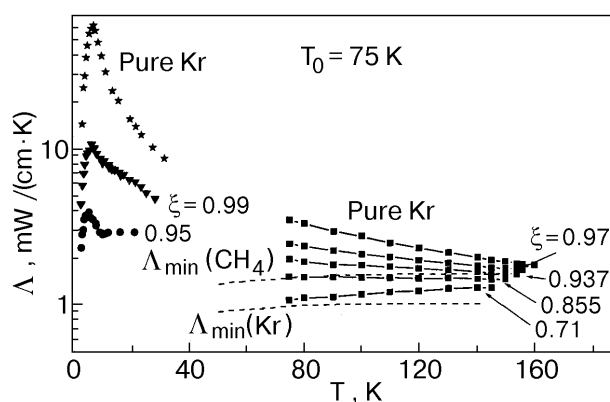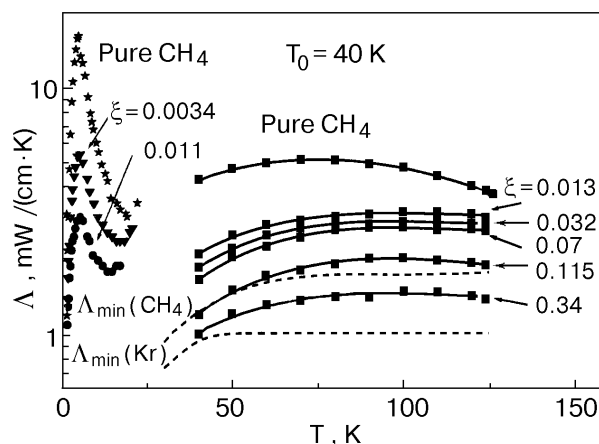

Fig. 4. Smoothed values of the isochoric thermal conductivity of pure Kr [11] and Kr with a CH_4 admixture, rescaled to $T_0 = 75$ K (■), together with low-temperature data [12]. The broken lines are the isochoric Λ_{min} of pure Kr and CH_4.

Fig. 5. Smoothed values of the isochoric thermal conductivity of pure CH_4 [13] and CH_4 with a Kr admixture, rescaled to $T_0 = 40$ K (■), together with low-temperature data [15]. The broken lines are the isochoric Λ_{min} of pure Kr and CH_4.
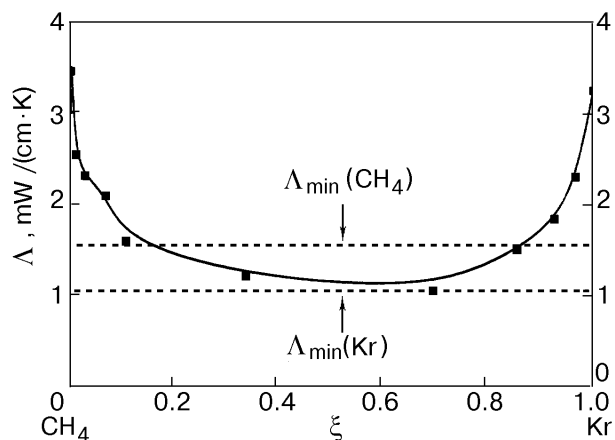
Fig. 6. The concentration dependence of the thermal conductivity of $(CH_4)_{1-\xi}Kr_\xi$ solid solutions at $T = 75$ K and $P = 0$. The horizontal lines are Λ_{min} of pure Kr and CH_4 under the same conditions.

Discussion

In the solidified inert gases Ar, Kr, and Xe the phonon–phonon interaction is the main mechanism determining the value and the temperature dependence of the thermal conductivity $\Lambda(T)$ at the Debye temperature and higher (He and Ne melt at temperatures much below Θ_D (Ref. 16, Chapter 11)). If the scattering is not too strong and the model of elastic waves is appropriate, the theory predicts that the isochoric thermal conductivity should vary as $\Lambda_V \propto 1/T$ at $T \geq \Theta_D$ [1–4,18]. However, experiments at constant volume revealed appreciable deviations from this dependence at the highest temperatures, with the conductivity varying slower than $1/T$ [11,16,19]. Such behavior implies an approach of the thermal conductivity toward its lower limit Λ_{min} [3,19]. The proximity of the thermal conductivity of solidified inert gases to Λ_{min} at premelting temperatures was first pointed out by Slack [4].

A characteristic peculiarity of molecular crystals is the presence of both translational and rotational motions of molecules in their lattice sites. For normal (orientationally ordered) molecular solids the intermolecular modes generally have a mixed translational-librational character and cannot be considered as independent. It is assumed, however, that separation can be made in orientationally ordered phases at low temperatures, and then collective translational vibrations (phonons) and rotational vibrations (librons) can be treated separately [20]. The contribution of librons to the heat transfer is assumed to be relatively small because the bands which are connected with the angular motion of the molecules are narrow. At the same time, the role of librons in scattering processes is important [20]. In orientationally disordered phases, however, the absence of orientational long-range order means that well-defined, librational modes cannot propagate through the crystal: they are always rapidly damped out [21]. The additional phonon scattering (beyond the phonon–phonon) may originate in the OD phases of molecular crystals due to the short-range fluctuations of the orientational order in the vicinity of the phase transition. For example, in solid CH_4 this additional scattering above the α–β transition temperature $T_{\alpha-\beta} = 20.4$ K is of the same magnitude as the phonon–phonon scattering [13,14]. However, it decreases rapidly when the temperature increases and practically disappears above 90 K, whereas the phonon–phonon scattering continues to increase. The competition of these two (phonon–phonon and phonon–rotational) mechanisms of scattering in the OD phase of solid CH_4 results in another high-temperature maximum of the thermal conductivity, in addition to the low-temperature one at 4.5 K. The models describing the phonon scattering on fluctuations of the orientational short-range order in solid methane were suggested in [14,22]. It has already been mentioned above that Λ_{meas} exceeds Λ_{min} by a factor of two to four in the OD phase of methane. The additional scattering mechanism due to Kr impurity (which is supposed to be very strong because of the big mass difference) decreases the thermal conductivity with increasing ξ to values which are between the predicted Λ_{min} for pure Kr and CH_4, calculated according to Eq. (1).

Defects of atomic dimensions weaken the temperature dependence of the lattice thermal conductivity caused by U-processes [3,23]. The theoretical consideration of point defect scattering in the framework of the Debye model at $T \geq \Theta_D$ is made with the assumption that the perturbation theory is valid at all frequencies and temperatures [18,23,24]. Point defects at small concentrations ($\xi < 0.05$) have to lead to an additional contribution to the thermal resistivity $W = 1/\Lambda$ of the crystal, which is independent of temperature [24]. The slowest variation in the limit of very strong point-defect scattering is $\Lambda \propto 1/T^{1/2}$ [25]. It has been already noted above that the thermal conductivity of Kr appears to approach its lower limit Λ_{min} at premelting temperatures (see Fig. 1). If Λ_{min} actually is the lower limit to the thermal conductivity of a lattice, the point-defect scattering should be different from that discussed above. Intuitively, one would expect that the contribution of small concentrations of point defects to the thermal resistivity should decrease with increasing temperature. In the case of very strong point-defect scatte-

ring Λ may coincide with Λ_{min} in a wide temperature range. To check this assumption the thermal resistivity of pure Kr and $(CH_4)_{1-\xi}Kr_\xi$ solid solutions with Kr prevailing is shown in Fig. 7 ($T_0 = 75$ K). It is seen clearly that the additional contribution of CH_4 impurities to the total thermal resistivity decreases with increasing temperature at all $\xi > 0.7$. At $0.85 \geq \xi \geq 0.7$ the thermal conductivity lies between the predicted Λ_{min} for pure Kr and CH_4, calculated according to Eq. (1) (see Fig. 4).

A quantitative description of the thermal conductivity of $(CH_4)_{1-\xi}Kr_\xi$ solid solutions with Kr prevailing ($\xi > 0.7$) is made by taking into consideration only U-processes and Rayleigh scattering. Phonon scattering at the excitations of the rotational motion of the methane molecules, which play an important role at low temperature [12], is expected to be weak at high temperatures. It was shown earlier that molecules undergo a almost free rotation in pure CH_4 at $T \sim 90$ K and higher [13], and that this kind of rotation does not lead to additional phonon scattering. For matrix isolated molecules in solidified inert gases the onset of almost free rotation takes place at lower temperatures [8].

The thermal conductivity can be described using the Debye model as

$$\Lambda(T) = 3nk_B v \left(\frac{T}{\Theta_D}\right)^3 \int_0^{\Theta_D/T} l(x) \frac{x^4 e^x}{(e^x - 1)^2}\, dx \ , \quad (2)$$

where $\Theta_D = v\,(\hbar/k_B)(6\pi^2 n)^{1/3}$ is the Debye temperature, v is the polarization-averaged sound velocity, and $l(x)$ is the phonon mean free path. At $T \geq \Theta_D$ the boundary scattering is negligible and the phonon mean free path is determined by the U-processes and Rayleigh scattering [18]:

$$l(x) = (l_{Rayl}^{-1} + l_{Umkl}^{-1})^{-1} \ , \quad (3)$$

where $x = vh/k_B T\lambda$, and λ is the phonon wavelength.

Frequently used expressions for the phonon mean free path resulting from the individual scattering mechanisms are

$$l_{Umkl}^{-1} = \frac{CT}{\lambda^2} \quad (4)$$

where

$$C = \frac{12\pi^3}{\sqrt{2}\ n^{1/3}} \frac{\gamma^2 k_B}{m v^2} \ , \quad (5)$$

and

$$l_{Rayl}^{-1} = \frac{4\pi^3 \Omega_0 \Gamma}{\lambda^4} \quad (6)$$

where

$$\Gamma = \xi\,(1 - \xi)\left[\frac{\Delta M}{M} + 2\gamma\frac{\Delta\Omega_0}{\Omega_0}\right]^2 . \quad (7)$$

Here γ is the Grüneisen parameter, taken as 2.5 for Kr and CH_4 [8,16], m is the atomic/molecular mass, and M and Ω_0 are the average atomic/molecular weight and volume respectively of the mixed crystals (for pure CH_4 $\Omega_0 = 5.18\cdot10^{-23}$ cm^3, $M = 16$, and for pure Kr $\Omega_0 = 4.73\cdot10^{-23}$ cm^3, $M = 83.8$), and ΔM and $\Delta\Omega_0$ are the atom/molecule weight and volume difference from their average values, respectively.

Expression (3) cannot apply when $l(x)$ becomes less than the interatomic spacing or shorter than the phonon wavelength. In that case a lower limit of the mean free path is reached. This problem has already been discussed for the case of U-processes only [3]. Let us extend this consideration to the case of combined U-processes and Rayleigh scattering.

i) Let us assume that the lower limit of the phonon mean free path is of the order of one-half of the phonon wavelength. In this case $l(x)$ is given by Eq. (3) when $l(x) \geq \alpha\lambda/2$ or otherwise by
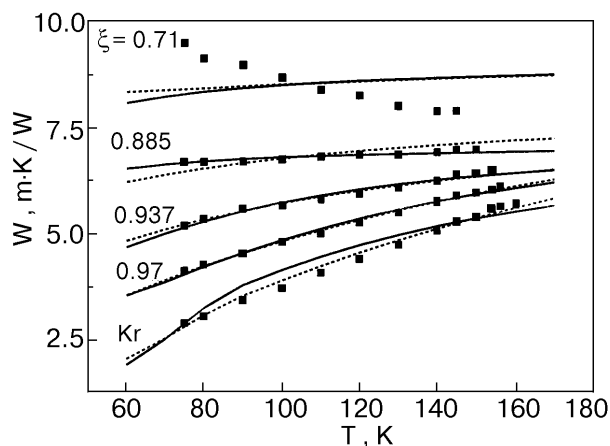
$$l(x) = \alpha\lambda/2 \ , \quad (8)$$

Fig. 7. The isochoric thermal resistivity of pure Kr and Kr with a CH_4 admixture, rescaled to $T_0 = 75$ K. The solid and dashed lines correspond to the best fit within the Debye model of the thermal conductivity according to i) and ii), respectively.

where α is some numerical coefficient of the order of unity which is assumed to be independent of T and λ. The crossover from behavior described by Eq. (3) to (8) occurs at the phonon wavelength λ_*, which is determined from

$$\left(\frac{CT}{\lambda_*^2} + \frac{B}{\lambda_*^4}\right)^{-1} = \alpha\,\frac{\lambda_*}{2}\,. \qquad (9)$$

This corresponds to the effective crossover temperature $\Theta_* = hv/k_B\lambda_*$. (It is supposed that $\Theta_* < \Theta_D$; otherwise $\Theta_* = \Theta_D$.) The thermal conductivity integral is broken into two parts:

$$\Lambda(T) = 3nk_Bv\left(\frac{T}{\Theta_D}\right)^3\left[\int_0^{\Theta_*/T} l(x)\frac{x^4e^x}{(e^x-1)^2}\,dx + \right.$$

$$\left. + \int_{\Theta_*/T}^{\Theta_D/T} \alpha\frac{\lambda}{2}\frac{x^4e^x}{(e^x-1)^2}\,dx\right]. \qquad (10)$$

In the high-temperature limit $T \geq \Theta_D$ when only the U-processes are in effect, $\Lambda(T) = A_1/T^2 + \Lambda'_{\min}$ [3,27], where A_1 is some numerical coefficient independent of the temperature, and $\Lambda'_{\min}$ is

$$\Lambda'_{\min} = 3\alpha\left(\frac{\pi}{6}\right)^{1/3} n^{2/3}k_Bv\left(\frac{T}{\Theta_D}\right)^2\int_0^{\Theta_D/T}\frac{x^3e^x}{(e^x-1)^2}\,dx\,. \qquad (11)$$

This expression for $\Lambda'_{\min}$ is identical to that predicted by Eq. (1) if the polarization-averaged speed of sound is used and it is assumed that $\alpha = 1$. In the case of strong phonon scattering caused by point defects (when $\Theta_* \ll \Theta_D$), the lower limit on the thermal conductivity is accurately found from Eq. (11).

ii) Let us assume that the lower limit of the phonon mean free path is of the order of the interatomic distance. In this case the phonon mean free path $l(x)$ is given by Eq. (3) when $l(x) \geq \alpha n^{-1/3}$ or otherwise by

$$l(x) = \alpha n^{-1/3}\,. \qquad (12)$$

The crossover from behavior described by Eq. (3) to (12) occurs at the phonon wavelength λ_*, which is determined from

$$\left(\frac{CT}{\lambda_*^2} + \frac{B}{\lambda_*^4}\right)^{-1} = \alpha n^{-1/3}\,. \qquad (13)$$

The effective crossing temperature is $\Theta_* = hv/k_B\lambda_*$. (It is supposed just as in previous case that $\Theta_* < \Theta_D$; otherwise $\Theta_* = \Theta_D$.) The thermal conductivity is again a sum of two integrals

$$\Lambda(T) = 3nk_Bv\left(\frac{T}{\Theta_D}\right)^3\left[\int_0^{\Theta_*/T} l(x)\frac{x^4e^x}{(e^x-1)^2}\,dx + \right.$$

$$\left. + \alpha n^{-1/3}\int_{\Theta_*/T}^{\Theta_D/T}\frac{x^4e^x}{(e^x-1)^2}\,dx\right]. \qquad (14)$$

In the high-temperature limit $T \geq \Theta_D$, when only the U-processes are in effect, $\Lambda(T) = A_2/T^{3/2} + \Lambda''_{\min}$ [3,27], where A_2 is some numerical coefficient, and $\Lambda''_{\min}$ is

$$\Lambda''_{\min} = 3\alpha n^{2/3}k_Bv\left(\frac{T}{\Theta_D}\right)^3\int_0^{\Theta_D/T}\frac{x^4e^x}{(e^x-1)^2}\,dx\,. \qquad (15)$$

In the case of strong phonon scattering by point defects (when $\Theta_* \ll \Theta_D$), the lower limit on the thermal conductivity is accurately found from Eq. (15). It can be shown easily that the ratio $\Lambda''_{\min}/\Lambda'_{\min} = 0.83$ at $T \geq \Theta_D$, for the same α.

iii) We consider also the case when the term $\alpha\lambda/2$ or $\alpha n^{-1/3}$ has simply been included in Eq. (3) for the phonon mean free path to eliminate a non-physical case when $l(x)$ becomes smaller than one-half the wavelength or than the interatomic distance:

$$l(x) = (l_{\text{Umkl}}^{-1} + l_{\text{Rayl}}^{-1})^{-1} + \alpha\lambda/2\,, \qquad (16)$$

$$l(x) = (l_{\text{Umkl}}^{-1} + l_{\text{Rayl}}^{1})^{-1} + \alpha n^{-1/3}\,, \qquad (17)$$

and then Eq. (2) is used to calculate the thermal conductivity [26]. In the high-temperature limit $T \geq \Theta_D$, this assumption leads to the expressions: $\Lambda = A_3/T + \Lambda'_{\min}$ and $\Lambda = A_4/T + \Lambda''_{\min}$ [27], where A_3 and A_4 are some numerical coefficients.

The computer fit using Eqs. (10), (14), (16) and (17) was performed for the isochoric thermal conductivity of pure Kr and $(CH_4)_{1-\xi}Kr_\xi$ solid solutions ($\xi = 0.97, 0.937, 0.855, 0.71$) for the isochores with $T_0 = 75$ K. The density was estimated by interpolation of experimental data. The sound velocity was calculated assuming that it changes linearly with the concentration from Kr [16] to CH_4 [8]. To

Table 4

Parameters of the Debye model fits for $(CH_4)_{1-\xi}Kr_\xi$ solid solutions for cases i) and ii)

ξ	$n \cdot 10^{-22}$, cm^{-3}	v, km/s	Γ_{calc}	i)		ii)	
				C, cm/K	α	C, cm/K	α
1	2.11	0.86	0	$1.07 \cdot 10^{-9}$	1.29	$0.95 \cdot 10^{-9}$	1.16
0.97	2.10	0.88	0.055	$1.17 \cdot 10^{-9}$	1.22	$1.07 \cdot 10^{-9}$	1.24
0.937	2.09	0.92	0.12	$2.03 \cdot 10^{-9}$	1.41	$1.63 \cdot 10^{-9}$	1.26
0.855	2.06	0.97	0.26	$3.5 \cdot 10^{-9}$	1.3	$3.8 \cdot 10^{-9}$	1.20
0.71	2.04	1.07	0.54	$6.2 \cdot 10^{-9}$	1.05	$4.5 \cdot 10^{-9}$	0.97

reduce the number of variable parameters, the coefficient B describing the Rayleigh scattering was calculated in accordance with Eqs. (6) and (7). The Debye model parameters used for fitting (n, v, Γ) and the C and α values obtained by fit for variants i) and ii) are shown in Table 4. When Eqs. (16) and (17) are used for the phonon mean free path, we obtain $\alpha \approx 0.3-0.4$ while elementary considerations lead to $\alpha \geq 1$. The coefficient C determining the intensity of the U-processes is in good agreement with low-temperature data [12], where it was evaluated as $1.5 \cdot 10^{-9}$ cm/K.

The fitting results are shown in Fig. 7. It is seen that both the variants describe well the behavior of the isochoric thermal conductivity of the solid solution, except for the concentration $\xi = 0.71$. In the case of pure Kr variant ii) ensures a somewhat better fit, as was discussed earlier for the isochore with $T_0 = 0$ K [27]. Roufosse and Klemens [3] preferred assumption ii) to i) for the following reason. Assumption i) means that the vibrational excitations can be described as waves. However, 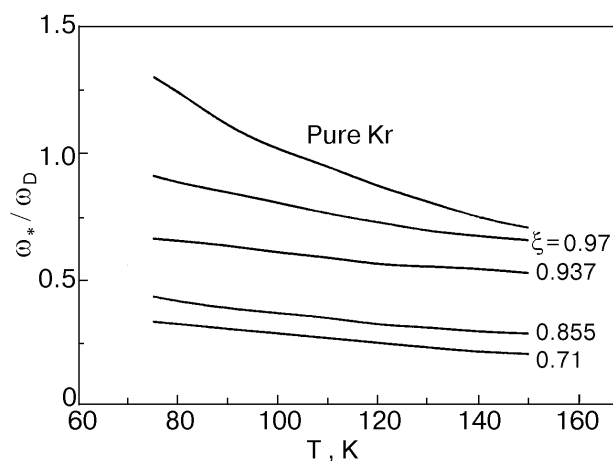when the wave picture is questioned, the alternative description assumes localized excitations that hop from site to site. The mean free path for those excitations is given by the interatomic distance.

This point of view may hold for amorphous materials as well, in which the heat transfer by low-frequency phonons is negligible at quite high (above 50 K) temperatures [28]. We should remember that in our case the model assumes a gradual change from pure extended-phonon thermal conductivity (a perfect crystal and low temperatures) to a heat transfer by localized excitations (a solid solution in the middle of composition range and high temperatures). We believe it is more reasonable to consider the vibrations localized in the $\lambda/2$ regions as the limiting case of the phonon picture (see [5,6]).

Figure 8 shows the temperature dependence ω_*/ω_D, where $\omega_* = 2\pi v/\lambda_*$ is the frequency at which the crossover from the wave picture to the picture of localized excitations occurs. Equation (10) actually describes the sum of contributions to the thermal conductivity resulting from extended phonons and localized excitations. Figure 9 presents the relative extended-phonon contribution to the
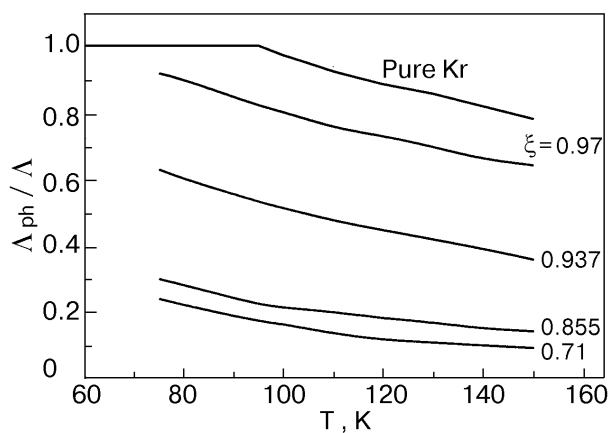

Fig. 8. The temperature dependence ω_*/ω_D, where $\omega_* = 2\pi v/\lambda_*$ is the frequency at which the crossover from the wave picture to the picture of localized excitations occurs.

Fig. 9. The relative extended-phonon contribution to the thermal conductivity of pure Kr and the $(CH_4)_{1-\xi}Kr_\xi$ solid solution.
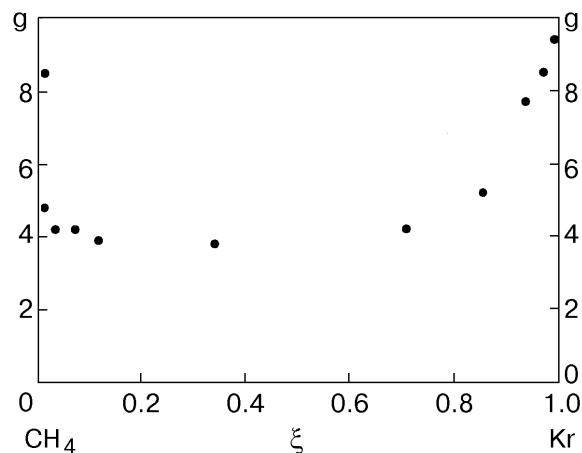
Fig. 10. The concentration dependence of the Bridgman coefficient $g = -(\partial \ln \Lambda / \partial \ln V)_T$ of the solid solution $(CH_4)_{1-\xi}Kr_\xi$ at $T = 90$ K.

thermal conductivity of pure Kr and the $(CH_4)_{1-\xi}Kr_\xi$ solid solution. It is seen that in Kr the thermal conductivity is of pure extended-phonon character up to about 90 K. As the CH_4 concentration grows, progressively more heat is transferred by the localized excitations, but even at the highest concentration (29%) and the highest temperatures (150 K) an appreciable part of the heat (about 10%) is transferred by the low-frequency extended phonons. The values of α vary from 1 to 1.4. This supports the view about the vibrations being localized in $\lambda/2$ regions as the limiting case of the phonon picture and the validity of Eq. (1) for prediction of the lower limit to the thermal conductivity of the crystalline lattice.

The concentration dependence of the Bridgman coefficient $g = -(\partial \ln \lambda / \partial \ln V)_T$ is shown in Fig. 10. It is seen that the value of g is highest for pure components and decreases strongly for solid solutions. The same behavior was also observed for mixed alkali-halide crystals [29], though the decrease in g was not such large. Small Bridgman coefficients $(g \approx 3{-}4)$ are typical for amorphous materials and strongly disordered crystals [30].

Conclusion

A gradual transition from the thermal conductivity of a highly perfect crystal to the minimum thermal conductivity Λ_{min} was observed at $T \geq \Theta_D$ in the $(CH_4)_{1-\xi}Kr_\xi$ solid solutions as the crystal becomes increasingly disordered. The qualitative description is given in the framework of Debye model of thermal conductivity, which takes into consideration the fact that phonon mean free path cannot decrease indefinitely. The concept of the

minimum thermal conductivity [3,4] gives a proper description of the isochoric thermal conductivity of the $(CH_4)_{1-\xi}Kr_\xi$ solid solution in the middle of composition range $0.2 < \xi < 0.8$.

Acknowledgments

1. P. B. Allen and J. L. Feldman, *Phys. Rev.* **B48**, 12581 (1993).
2. P. Sheng, M. Zhou, and Z. Zhang, *Phys. Rev. Lett.* **72**, 234 (1994).
3. M. C. Roufosse and P. G. Klemens, *J. Geophys. Res.* **79**, 703 (1974).
4. G. A. Slack, in: *Solid State Physics*, vol. 34, F. Seitz and D. Turnbull (eds.), Academic Press, New York (1979).
5. D. G. Cahill and R. O. Pohl, *Solid State Commun.* **70**, 927 (1989).
6. D. G. Cahill, S. K. Watson, and R. O. Pohl, *Phys. Rev.* **B46**, 6131 (1992).
7. V. G. Manzhelii, A. I. Prokhvatilov, I. Ya. Minchina, and L. D. Yantsevich, *Handbook of Binary Solutions of Cryocrystals*, Begell House Inc., N. Y., Wallingford, UK (1996).
8. V. G. Manzhelii, A. I. Prokhvatilov, V. G. Gavrilko, and A. P. Isakina, *Structure and Thermodynamic Properties of Cryocrystals*, Begell House Inc., N.Y., Wallingford, UK (1999).
9. I. N. Krupskii and V. G. Manzhelii, *Sov. Phys. JETP* **55**, 2075 (1968).
10. P. Korpium, J. Moser, F. J. Piezinger, and E. Lusher, in: *Phonon Scattering in Solids*, L. J. Challis, V. W. Rampton, and A. F. G. Wyatt (eds.), Plenum Press, N.Y., and London (1975), p. 377.
11. A. I. Bondarenko, V. G. Manzhelii, V. A. Popov, M. A. Strzhemechnyi, and V. G. Gavrilko, *Fiz. Nizk. Temp.* **86**, 1215 (1982) [*Sov. J. Low Temp. Phys.* **8**, 617 (1982)].
12. V. V. Dudkin, B. Ya. Gorodilov, A. I. Krivchicov, and V. G. Manzhelii, *Fiz. Nizk. Temp.* **26**, 1023 (2000) [*Low Temp. Phys.* **26**, 762 (2000)].
13. V. A. Konstantinov V. G. Manzhelii, V. P. Revyakin, and S. A. Smirnov, *Physica* **B262**, 421 (1999).
14. V. G. Manzhelii and I. N. Krupskii, *Fiz. Tverd. Tela* **10**, 284 (1968).
15. B. Ya. Gorodilov, V. V. Sumarokov, P. Stachowiak, and A. Jezovski, *Phys. Rev.* **B58**, 3089 (1998).
16. *Rare Gas Solids*, v. II, M. L. Klein and J. A. Venables (eds.), Academic Press, London − N. Y. (1977).
17. V. A. Konstantinov, S. A. Smirnov, and V. P. Revyakin, *Prib. Tekh. Exp.* **42**, 145 (1999) [*Instrum. Exp. Tech. (USSR)* **42**, 133 (1999)].
18. R. Berman, *Thermal Conduction in Solids*, Oxford, Clarendon Press (1976).
19. V. A. Konstantinov, V. G. Manzhelii, M. A. Strzhemechnyi, and S. A. Smirnov, *Fiz. Nizk. Temp.* **14**, 90 (1988) [*Sov. J. Low Temp. Phys.* **14**, 48 (1988)].
20. V. G. Manzhelii, V. B. Kokshenev, L. A. Koloskova, and I. N. Krupskii, *Fiz. Nizk. Temp.* **1**, 1302 (1975) [*Sov. J. Low Temp. Phys.* **1**, 624 (1975)].

21. B. M. Powell and G. Dolling, *Can. J. Chem.* **66**, 897 (1998).
22. H. Yasuda, *J. Low Temp. Phys.* **31**, 223 (1978).
23. P. G. Klemens, *Phys. Rev.* **119**, 507 (1960).
24. V. S. Oscotskii and L. A. Smirnov, *Defects in Crystals and Heat Conduction*, Nauka, Leningrad (1972) [in Russian].
25. L. A. Turk and P. G. Klemens, *Phys. Rev.* **B9**, 4422 (1974).
26. J. R. Olson, R. O. Pohl, J. W. Vandersande, A. Zoltan, T. R. Anthony, and W. F. Banholzer, *Phys. Rev.* **B47**, 14850 (1993).
27. V. A. Konstantinov, *J. Low Temp. Phys.* **122**, 459 (2001).
28. M. S. Love and A. S. Anderson, *Phys. Rev.* **B42**, 1845 (1990).
29. D. Gerlich, *J. Phys.* **C20**, 5479 (1987).
30. R. G. Ross, P. A. Andersson, B. Sundqvist, and G. Backstrom, *Rep. Prog. Phys.* **47**, 1347 (1984).